absorption method. The growth of europium on palladium surfaces has also been investigated using atomic emission spectroscopy.

The use of inductively coupled plasma–atomic emission spectroscopy (ICP-AES) has been applied to the analysis of traces of certain rare earth metals in highly pure rare earth matrices and to the levels of approximately 25 impurities in sintered electronic ceramics.

The impurity levels and profiles from the surface into the bulk sample have been probed using a combination of secondary-ion mass spectrometry and electrothermal atomic absorption spectroscopy in composite materials such as CdZnTe.

See also: **Atomic Absorption, Methods and Instrumentation; Atomic Absorption, Theory; Atomic Emission, Methods and Instrumentation; Atomic Spectroscopy, Historical Perspective; Inductively Coupled Plasma Mass Spectrometry, Methods; Materials Science Applications of X-Ray Diffraction; X-Ray Fluorescence Spectroscopy, Applications.**

Further reading

Bertran F, Gourieux T, Krill G, Alnot M, Ehrhardt JJ and Felsch W (1991) Growth of Eu on Pd(111) – AES, photoemission and RHEED studies. *Surface Science* **245**: L163–L169.

Daskalova N, Velichkov S, Krasnobaeva N and Slavova P (1992) Spectral interferences in the determination of traces of scandium, yttrium and rare earth elements in pure rare earth matrices by inductively coupled plasma atomic emission spectrometry. *Spectrochimica Acta* **B47**: E1595–E1620.

Gerardi C, Milella E, Campanella F and Bernadi S (1996) SIMS-ETAAS characterization of background impurities in CdZnTe bulk samples. *Material Science Forum* **203**: 273–278.

Gupta PK and Ramchandran R (1991) Indirect atomic absorption spectrometric determination of phosphorus in high purity electronic grade silicon using bismuth phosphomolybdate complex. *Microchemical Journal* **44**: 34–38.

Morvan D, Amouroux J and Claraz P (1984) Analysis of electronic and solar grade silicon by atomic emission spectroscopy from inductively coupled plasma. *Progress in Crystal Growth and Characterization* **8**: 175–180.

Uwamino Y, Morikawa H, Tsuge A, Nakane K, Iida Y and Ishizuka T (1994) Determination of impurities in sintered electronic ceramics by inductively coupled plasma atomic emission spectrometry. *Microchemical Journal* **49**: 173–182.

Ellipsometry

GE Jellison Jr, Oak Ridge National Laboratory, Oak Ridge, TN, USA

ELECTRONIC SPECTROSCOPY
Applications

Ellipsometry is a technique often used to measure the thickness of a thin film. Generally speaking, the measurement is performed by polarizing the incident light beam, reflecting it off a smooth sample surface at a large oblique angle and then re-polarizing the light beam before the intensity of the light beam is measured. Since the process of reflecting light off a smooth sample surface generally changes linearly polarized light into elliptically polarized light, the technique has been called 'ellipsometry'.

The earliest ellipsometry measurements (ca 1890) were used to determine the optical functions (refractive index n and extinction coefficient k, or equivalently, absorption coefficient α) for several materials. In the 1940s it was discovered that a single-wavelength nulling ellipsometry measurement could be used to determine the thickness of certain thin films very accurately. Since that time, single-wavelength ellipsometry has evolved to be the standard of thickness measurement for several industries, including the semiconductor industry.

Ellipsometry experiments produce values that are not useful by themselves: computers must be used to obtain useful quantities such as thin-film thickness or the optical functions of materials. The advent of modern computers has resulted in the invention of several spectroscopic ellipsometers and the creation of more realistic analysis programs required to understand spectroscopic ellipsometry data.

Any ellipsometer (see **Figure 1**) consists of five elements: (1) a light source, (2) a polarization state generator (PSG), (3) a sample, (4) a polarization state detector (PSD), and (5) a light detector. The light source can be a monochromatic source, such as from a laser, or a white light source, such as from a xenon or mercury arc lamp. The PSG and

PSD are optical instruments that change the polarization state of a light beam passing through them and they contain optical elements such as polarizers, retarders and photoelastic modulators. In most ellipsometry experiments, light from the PSG is reflected from the sample surface at a large angle of incidence ϕ. Spectroscopic ellipsometers use a white light source and a monochromator (either before the PSG or after the PSD) to select out specific wavelengths. Some spectroscopic ellipsometers image the white light from the PSD onto a detector array, thereby allowing the whole spectrum to be collected simultaneously.

Any ellipsometer will only measure characteristics of the light reflected from or light transmitted through the sample. Ellipsometers do not measure film thicknesses or optical functions of materials, although these parameters can often be inferred very accurately from the ellipsometry measurements. Data analysis is an essential part of any ellipsometry experiment.

Polarization optics

Several optical elements will change the polarization state of a light beam interacting with them. Linear polarizers (see **Figure 2A**) transmit only one polarization of the light beam; the azimuthal angle of the polarizer will determine the azimuthal angle of the light polarization. The best linear polarizers in the visible part of the spectrum are prism polarizers made from birefringent crystals such as calcite, magnesium fluoride or quartz, which have refractive indices that depend upon the direction in the material.

Retarders or compensators (see **Figure 2B**) are another common type of optical element used in ellipsometers. In combination with a polarizer, a retarder can produce circularly or elliptically polarized light if the direction of the linear polarization is not parallel to a major axis in the retarder. Static retarders, such as quarter-wave or half-wave plates produces a fixed amount of retardation at a fixed wavelength. Circularly polarized light can be produced from a polarizer–quarter-wave retarder pair if the light polarization is $\pm 45°$ with respect to the fast axis of a retarder.

Another common retarding element used in spectroscopic ellipsometers is the photoelastic modulator (PEM), shown schematically in **Figure 2C**. The drive element is a crystal quartz bar, which is cut so that an a.c. voltage V applied to the front and back faces causes the bar to vibrate along its long axis at the frequency of V. The optical element is a bar made of fused quartz that is placed in intimate contact with the crystal quartz bar so that it vibrates at the same frequency. Both bars are sized so that the vibrations are resonant, making the frequency of the PEM extremely stable. A polarizer–PEM pair produces dynamically elliptically polarized light if the polarizer

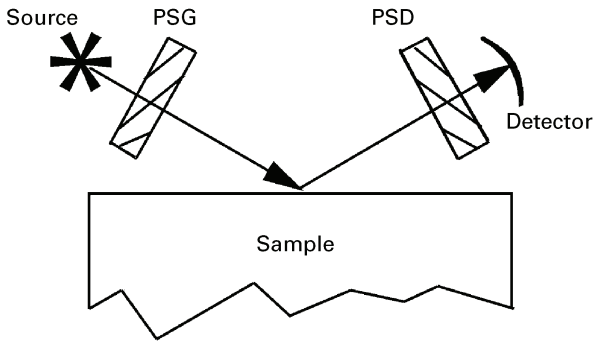

Figure 1 Schematic diagram of an ellipsometer. The PSG is the polarization state generator and the PSD is the polarization state detector.

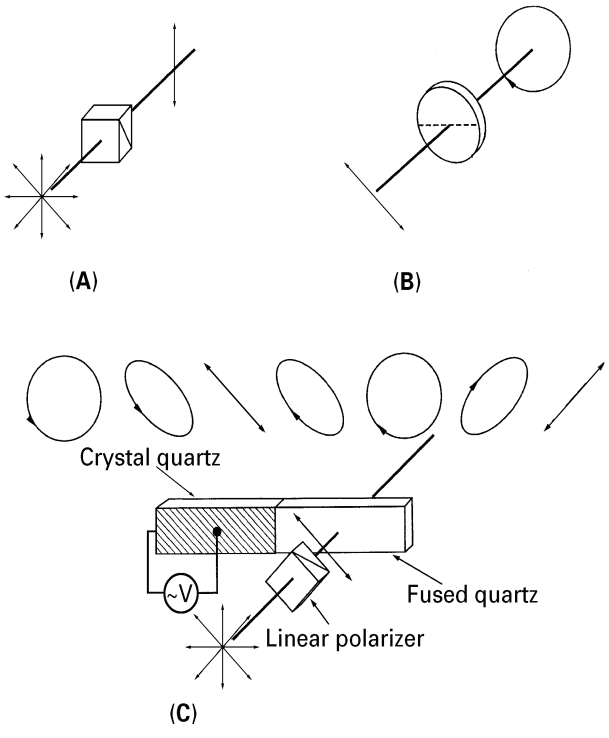

Figure 2 Several optical elements used in ellipsometers that alter the polarization state of a light beam passing through them. (A) A linear polarizer, which transforms any light beam (polarized or unpolarized) to linearly polarized light. (B) A retarder, which transforms linearly polarized light to elliptically polarized light. In certain cases, the light can be circularly polarized. (C) A photoelastic modulator, which changes linearly polarized light into dynamically elliptically polarized light.

is not lined up with the vibration axis of the PEM; generally, the polarization state of the emergent light beam will cycle through linearly polarized, circularly polarized and elliptically polarized states.

The Stokes vector representation of light polarization has often been used for ellipsometry measurements. (Another representation is the Jones vector representation, of which details can be found in the book by Azzam and Bashara listed under Further reading). In the Stokes representation, the polarization state of a light beam is given by its four-element Stokes vector,

$$\boldsymbol{S} = \begin{bmatrix} I_0 \\ Q \\ U \\ V \end{bmatrix} = \begin{bmatrix} I_0 \\ I_0 - I_{90} \\ I_{45} - I_{-45} \\ I_{\mathrm{rc}} - I_{\mathrm{lc}} \end{bmatrix} \qquad [1]$$

All the elements of the Stokes vector are intensities and therefore are real. The total intensity is I_0, while I_0, I_{90}, I_{45}, and I_{-45}, are the intensities of linearly polarized light at 0°, 90°, 45°, and −45°, respectively. The fourth element of the Stokes vector V is the difference between the intensities of right circularly polarized light I_{rc}, and left circularly polarized light I_{lc}. A linear polarizer can only transform a light beam into a linear polarization state; therefore the fourth element of the Stokes vector for linearly polarized light will be $V = 0$. Generally, a retarding optical element is needed to transform the polarization state of a light beam to one where $V \neq 0$. The Stokes representation can also represent partially polarized light. In general,

$$I_0 \geq \sqrt{Q^2 + U^2 + V^2} \qquad [2]$$

where the equality holds when the light beam is totally polarized.

Each optical element must transform the polarization state from one four-element vector to another four-element vector; therefore, optical elements are represented by 4 × 4 Mueller matrices, where all the elements are real. The intensity of the light beam passing through an ellipsometer can therefore be written using matrix notation as

$$I = \boldsymbol{S}_{\mathrm{PSD}}^{T}\, \mathbf{M}\, \boldsymbol{S}_{\mathrm{PSG}} \qquad [3]$$

where $\boldsymbol{S}_{\mathrm{PSG}}$ is the Stokes vector representing the polarization state for light coming from the PSG, $\mathbf{M}$ is the Mueller matrix for the light interaction with the sample, and $\boldsymbol{S}_{\mathrm{PSD}}^{\mathrm{T}}$ is the transpose of the Stokes vector representing the effect of the PSD. In the most general case, 16 elements are required to describe the light interaction with a sample. Fortunately, many of these elements are normally 0 or equal to another element in $\mathbf{M}$. Since detectors can only measure the light intensity coming from an instrument, Equation [3] emphasizes the fact that ellipsometers can only measure elements of $\mathbf{M}$.

Ellipsometry data analysis

Ellipsometry measurements are not useful by themselves but can be extremely useful if the measurements are interpreted with an appropriate model. Ultimately, ellipsometry results are always model dependent. Fortunately, the physics of light reflection from surfaces is well understood, and very detailed and accurate models can be made using classical electromagnetic theory based on the Maxwell equations.

Figure 3 shows a schematic of light reflection from a sample surface. The light beam is incident upon the sample surface at an angle of incidence ϕ. The specularly reflected beam comes from the sample surface, also at angle ϕ. The incident and reflected beams define a plane, called the plane of incidence. This in turn defines two polarization directions: p for the light polarization parallel to the plane of incidence (in the plane of the paper), and s for the light polarization perpendicular to the plane of incidence (perpendicular to the plane of the paper). All azimuthal angles are defined with respect to the plane of incidence, where positive rotations are defined as clockwise rotations looking from the light source to the detector.

If the sample surface is isotropic and has no film or other overlayer ($d = 0$ in **Figure 3**), then one can use the Maxwell equations to calculate the complex reflection coefficients:

$$r_{\mathrm{p}} = \frac{N_{\mathrm{s}} \cos(\phi_0) - N_0 \cos(\phi_{\mathrm{s}})}{N_{\mathrm{s}} \cos(\phi_0) + N_0 \cos(\phi_{\mathrm{s}})} \qquad [4a]$$

$$r_{\mathrm{s}} = \frac{N_0 \cos(\phi_0) - N_{\mathrm{s}} \cos(\phi_{\mathrm{s}})}{N_0 \cos(\phi_0) + N_{\mathrm{s}} \cos(\phi_{\mathrm{s}})} \qquad [4b]$$

In Equations [4], N_0 and N_{s} ($= n_{\mathrm{s}} + \mathrm{i}k_{\mathrm{s}}$, where n_{s} is the refractive index and k_{s} is the extinction coefficient) are the complex indices of refraction for the ambient (usually air, where $N_0 = 1$) and the

substrate, respectively. The quantities ϕ_0 and ϕ_s are complex angles, determined from the Snell law [$N_0 \sin(\phi_0) = N_s \sin(\phi_s)$]. The reflection ratios r_p and r_s are complex, indicating that light reflected from a surface will generally undergo a phase shift.

If the sample near-surface region consists of a single film (see **Figure 3**), the composite reflection coefficients can be calculated from the Airy formula:

$$r_{s,p} = \frac{r_{1\,s,p} + r_{2\,s,p} e^{-2ib}}{1 + r_{1s,p}\, r_{2\,s,p}\, e^{-2ib}} \qquad b = \frac{2\pi d N_f \cos(\phi_f)}{\lambda} \quad [5]$$

where d is the thickness of the film, N_f is the complex refractive index of the film, and ϕ_f is the complex angle within the film defined by the Snell law. The quantities $r_{1s,p}$ and $r_{2s,p}$ are the complex reflection coefficients calculated using Equations [4a] and [4b] for the air–film interface and the film–substrate interface, respectively.

Reflections from more complicated layer structures can be calculated using matrix methods. If all the media in the calculation are isotropic, the matrix formulation of Abelés (using 2×2 complex matrices) can be used to calculate the composite r_s and r_p.

If any of the media are birefringent, many of the implicit assumptions made above are no longer valid. For example, for isotropic media the s and p polarization states represent eigenmodes of the reflection; that is, if the incoming light is pure s or p polarized, then the reflected light will be pure s or p polarized. If any of the media in the sample are birefringent, this assumption is no longer generally valid. As a result, one must also calculate the cross-polarization coefficients r_{sp} and r_{ps} as well as $r_{ss} \equiv r_s$ and $r_{pp} \equiv r_p$. If $r_{sp} \neq 0$ or $r_{ps} \neq 0$, the 2×2 matrix methods must be replaced by more complicated 4×4 matrix methods.

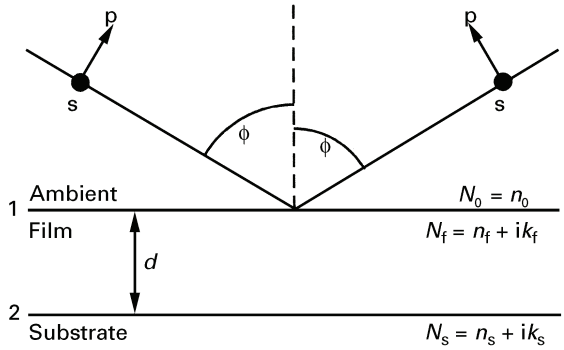

Figure 3 A schematic diagram of light reflecting from a sample surface. The s and p vectors indicate the direction of s and p polarized light, as defined by the plane of incidence. The angle of incidence is ϕ, and N_0, N_f and N_s are the complex refractive indices of the ambient, film and substrate, respectively.

Up to this point, a clear distinction has been drawn between the parameters measured by an ellipsometer (the sample Mueller matrix $\mathbf{M}$) and the calculated parameters obtained from classical electromagnetic theory, which can be expressed as elements of the sample Jones matrix:

$$\mathbf{J} = \begin{bmatrix} r_{pp} & r_{ps} \\ r_{sp} & t_{ss} \end{bmatrix} \quad [6]$$

Fortunately, the two representations are related, so long as it can be assumed that the sample does not depolarize the incident light beam. In this case, a Mueller–Jones matrix $\mathbf{M}_{MJ}$ can be calculated from the elements of the Jones matrix (Eqn [6]),

$$\mathbf{M}_{MJ} = \mathbf{A}\,(\mathbf{J} \otimes \mathbf{J}^*)\,\mathbf{A}^{-1} \quad [7a]$$

where

$$\mathbf{A} = \begin{bmatrix} 1 & 0 & 0 & 1 \\ 1 & 0 & 0 & -1 \\ 0 & 1 & 1 & 0 \\ 0 & -i & i & 0 \end{bmatrix} \quad [7b]$$

For isotropic samples ($r_{sp} = r_{ps} = 0$), the normalized sample Mueller–Jones matrix is given by

$$\mathbf{M} = \mathbf{M}_{MJ} = \begin{bmatrix} 1 & -N & 0 & 0 \\ -N & 1 & 0 & 0 \\ 0 & 0 & C & S \\ 0 & 0 & -S & C \end{bmatrix} \quad [8a]$$

where

$$N = \cos(2\psi) \quad [8b]$$

$$S = \sin(2\psi)\sin(\Delta) \quad [8c]$$

$$C = \sin(2\psi)\cos(\Delta) \quad [8d]$$

$$\rho = \frac{r_p}{r_s} = \tan(\psi)e^{i\Delta} = \frac{C + iS}{1 + N} = \rho_r + i\rho_i \quad [8e]$$

The angles ψ and Δ are the traditional ellipsometry angles, and are the naturally measured parameters for nulling ellipsometers (see below). The matrix $\mathbf{M}$ simplifies considerably when the sample is isotropic: $\mathbf{M}$ is block-diagonal, with eight elements equal to 0, and

only two parameters (such as $\rho = \rho_r + i\,\rho_i$ or ψ and Δ) are needed to specify **M**, since $N^2 + S^2 + C^2 = 1$.

For birefringent samples, $r_{sp} \neq r_{ps} \neq 0$, and the off-block diagonal elements of **M** are no longer 0, nor are the on-block diagonal elements of **M** so simply defined. However, Equation [7a] is still valid as long as the sample is nondepolarizing. In this case, six parameters are required to specify all 16 elements of the normalized sample Mueller matrix, given by Equation [8e] and

$$\rho_{ps} = \frac{r_{ps}}{r_{ss}} = \tan(\psi_{ps})e^{i\Delta_{ps}} = \frac{C_{ps} + iS_{ps}}{1 + N} \qquad [8f]$$

$$\rho_{sp} = \frac{r_{sp}}{r_{ss}} = \tan(\psi_{sp})e^{i\Delta_{sp}} = \frac{C_{sp} + iS_{sp}}{1 + N} \qquad [8g]$$

Up to now, we have assumed that no optical element depolarizes the light. Usually, this is true, but there are some cases where depolarization must be considered. (1) If the input light beam illuminates an area of the sample where the film thickness(es) is (are) not uniform, quasi-depolarization can occur. (2) If the sample substrate is transparent, then light reflecting from the back surface will contribute an intensity component to the light beam entering the PSD that is not phase-related to the light reflected from the front face and the light beam will be quasi-depolarized. (3) If the sample is very rough, then some of the light reaching the PSD will not have an identifiable polarization state or cross-polarization can occur in nominally isotropic systems. All of these effects invalidate the Mueller–Jones matrix representation of the sample surface shown in Equation [7a].

Types of ellipsometers

There are many different kinds of ellipsometers, some of which are shown schematically in **Figure 4**. All ellipsometers measure one or more quantities that can be related to the complex reflection coefficient ratio ρ shown in Equations [8].

Nulling ellipsometer

The oldest and most common type of ellipsometer is the nulling ellipsometer, shown schematically in **Figure 4A**. The light source for a modern nulling ellipsometer is usually a small laser, but other monochromatic sources can also be used. The PSG is a polarizer–retarder pair, and the PSD is a linear polarizer, historically called the analyser. If the quarter-wave plate is oriented at 45° with respect to the plane of incidence, the intensity of the light beam incident upon the detector is given by

$$I = I_0[1 - N\cos(2\theta_a) + \sin(2\theta_a)(C\sin(2\theta_p) + S\cos(2\theta_p))] \qquad [9]$$

where θ_p and θ_a are the azimuthal angles of the polarizer and analyser, respectively, and N, S and C are the quantities given in Equations [8]. The intensity given in Equation [9] has a null at two sets of angles: $(2\theta_p, \theta_a) = (270° - \Delta, \psi), (90° - \Delta, 180° - \psi)$. Therefore, nulling ellipsometry measurements are made by rotating the PSG polarizer and the PSD polarizer (analyser) until the light intensity reaching the detector is a minimum. The angles ψ and Δ are determined from the azimuthal angles of the PSG and PSD polarizers.

The nulling ellipsometer is one of the simplest ellipsometers and it is capable of very accurate measurements with proper calibration. However, it normally uses a single-wavelength source and it is not easily made spectroscopic. Moreover, measurement times are slow, so this type of instrument is not useful for spectroscopic ellipsometry or for fast time-resolved measurements.

Rotating analyser ellipsometer (RAE)

The most common type of spectroscopic ellipsometer is the rotating analyser (or rotating polarizer) ellipsometer, shown schematically in **Figure 4B**. The PSG is a linear polarizer, as is the PSD, and one of the optical elements (the analyser in **Figure 4B**) is physically rotated, making the light intensity at the detector a periodic function of time. For an analyser (PSD) rotating at an angular frequency of ω and with the polarizer (PSG) set at an azimuthal angle of θ_p, the intensity is given by

$$I(t) = I_0[1 + \alpha\cos(2\omega t + \delta_c) + \beta\sin(2\omega t + \delta_c)] \qquad [10a]$$

where

$$\alpha = \frac{\cos(2\theta_p) - N}{1 - N\cos(2\theta_p)} \qquad [10b]$$

$$\beta = \frac{C\sin(2\theta_p)}{1 - N\cos(2\theta_p)} \qquad [10c]$$

The quantity δ_c is a constant phase shift. The coefficients α and β can be determined using demodulation techniques or Fourier analysis. Normally, $\theta_p = 45°$, where $\alpha = -N$, and $\beta = C$.

In its normal form, the RAE includes only polarizers, although a retarder can be added to either the PSG or the PSD. If only polarizers are used, this instrument is very easy to make spectroscopic, since no optical component other than the sample is wavelength dependent. Furthermore, the measurement time depends principally on the rotation speed of the rotating element. For a rotation speed of 100 Hz, measurements can be completed in 40 ms. In some configurations of the rotating polarizer ellipsometer, a spectrograph is placed after the PSD and the light is detected by a photodiode array. This ellipsometer can collect an entire spectrum with a single series of measurements, typically taking about 1 s to collect and analyse each spectrum.

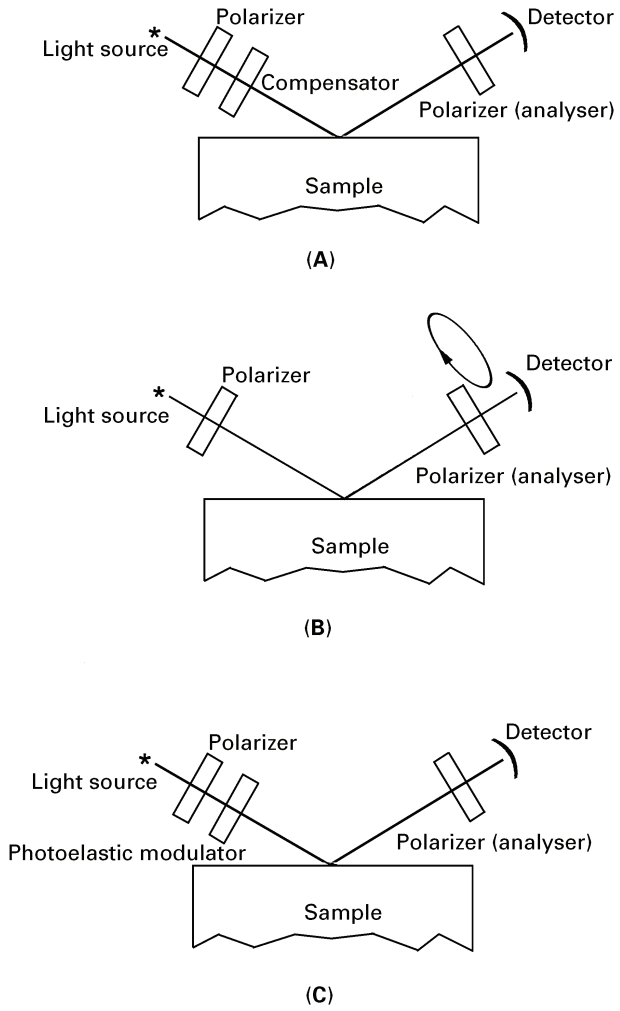

Figure 4 Schematic diagrams of three ellipsometers in common use. (A) The nulling ellipsometer, which normally uses monochromatic light. (B) The rotating analyser ellipsometer. (C) The polarization modulation ellipsometer.

The RAE measures two quantities, N and a linear combination of C and S. If there is no retarder, the RAE measures N and C, and will therefore be subject to large errors in Δ if Δ is near 0° or 180° and an uncertainty of the sign of Δ. The use of a quarter-wave retarder shifts the inaccuracy in Δ to the regions near ±90°.

Photoelastic modulator ellipsometer (PME)

Another common spectroscopic ellipsometer is based on the photoelastic modulator (PEM), shown in **Figure 4C**. Normally, the PSG consists of a polarizer–PEM pair, where the polarizer is oriented at 45° with respect to the vibration axis of the PEM (see **Figure 2C**). The intensity of the light arriving at the detector is a function of time given by

$$I(t) = I_0[I_{dc} + I_X \sin(A\sin(\omega t)) + I_Y \cos(A\sin(\omega t))] \quad [11a]$$

where

$$I_{dc} = 1 - N\cos(2\theta_a) \quad [11b]$$

$$I_X = S\sin(2\theta_a) \quad [11c]$$

$$I_Y = \sin(2\theta_m)\,[\cos(2\theta_m) - N] - C\cos(2\theta_m)\sin(2\theta_a) \quad [11d]$$

The quantity A is the Bessel angle of the PEM modulation, and is proportional to the amplitude of modulation; normally, this is set at 2.4048 radians. The frequency of the PEM is denoted by $2\pi\omega$, and is normally ~50 kHz. The quantities θ_m and θ_a are the azimuthal angles of the modulator and the PSD polarizer, respectively.

The time dependence of the light intensity from the PME is considerably more complicated than that from the RAE, since the basis functions are $\sin(A\sin(\omega t))$ and $\cos(A\sin(\omega t))$, rather than $\sin(\omega t)$ and $\cos(\omega t)$ as for the RAE. However, these functions can be expressed in terms of a Fourier–Bessel infinite series:

$$\sin(A\sin(\omega t)) = 2\sum_{k=1}^{\infty} J_{2k-1}(A)\sin((2k-1)\omega t) \quad [12a]$$

$$\cos(A(\sin(\omega t)) = J_0(A) + 2\sum_{k=1}^{\infty} J_{2k}\,(A)\sin(2k\omega t) \qquad [12b]$$

Therefore, a demodulation or Fourier analysis of the waveform of Equation [11a] can also be used to get the coefficients I_X and I_Y.

The PME is more complicated than the RAE, since the modulation amplitude of the PEM must be calibrated and its small but significant static retardation measured at all wavelengths used. Furthermore, the frequency of the PEM is about 500 times faster than the rotation speed of the RAE; this improves the time resolution to ~1 ms, but requires faster electronics for data collection. In its normal configuration discussed above, the PME can measure S and either N or C. However, if the PSD polarizer is replaced with a Wollaston prism polarizer and both channels are detected (measuring a total of four quantities), then it is possible to measure N, S, and C simultaneously. This implementation is called the two-channel spectroscopic polarization modulation ellipsometer (2C-SPME).

Other configurations

The ellipsometer configurations discussed above are particularly useful if the sample is isotropic. If the sample is anisotropic, then many of the simplifications used above are not valid, and many more measurements must usually be made, since the normalized sample Mueller matrix contains six independent quantities. One such implementation is the two-modulator generalized ellipsometer (2-MGE) which uses two PEMs operating at different frequencies. The 2-MGE is spectroscopic and is capable of measuring all six independent elements of the sample Mueller matrix simultaneously. Other configurations are discussed in the review article by Hauge.

Application: Silicon dioxide films on silicon

One of the most useful applications of ellipsometry has been the routine measurement of silicon dioxide (SiO_2) film thicknesses grown on silicon. Since the refractive index of SiO_2 is well known, and does not depend significantly on film deposition technique, nulling ellipsometry measurements are usually sufficient to determine film thickness.

Figure 5 shows a plot of ψ versus Δ for thin-film SiO_2 grown on silicon for a wavelength of 633 nm (the wavelength of a HeNe laser). The angle of incidence used for the calculation was 70°, the film

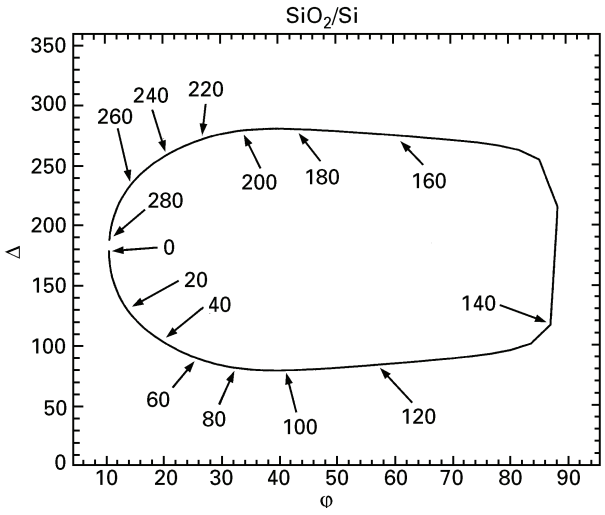

Figure 5 The ψ–Δ trajectory for a thin film of SiO_2 on silicon. The angle of incidence $\phi = 70°$, $n_f = 1.46$, $N_s = 3.86 + i0.018$, and the wavelength $\lambda = 633$ nm (HeNe laser).

refractive index $n_f = 1.46$, and the complex refractive index of silicon $N_s = n_s + ik_s = 3.86 + i\,0.018$. This plot shows the trajectory that ψ–Δ follows as the film thickness increases from zero to ~280 nm, where the position along the trajectory for several thicknesses is noted in the figure. For zero film thickness, the value of Δ is very close to 0° or 180°, owing to the very small value of k_s. If other film refractive indices were included in this plot, it would be seen that they would converge to this point. It is therefore very difficult to determine the refractive index and the thickness of a very thin film from ellipsometry measurements. Note that the curve comes around on itself near 283 nm. Therefore, any ellipsometry measurement of SiO_2/Si can only be used to determine the film thickness modulo the repeat thickness (283 nm). For film thicknesses from 140 to 160 nm, the measurements are very sensitive to film thickness, crossing the $\Delta = 180°$ point for a thickness of 141.5 nm (half the repeat thickness).

The same data are plotted in a different manner in **Figure 6**. Here, the complex ρ ($= \tan(\psi)\, e^{i\Delta}$, see Equation [8e]) is plotted versus film thickness. Near zero thickness, $\mathrm{Im}(\rho)$ (which is proportional to $\sin(\Delta)$) is very small. As the thickness approaches 140 nm, $-\mathrm{Re}(\rho)$ gets very large and $\mathrm{Im}(\rho)$ changes sign ($\mathrm{Im}(\rho) = 0$ at half the repeat thickness); this corresponds to the region of large ψ in **Figure 5**, with the change in the sign of $\mathrm{Im}(\rho)$ corresponding to Δ going through 180°. Again, the value of ρ repeats itself after 283 nm.

Figures 7A–C show the measured values of of ρ for three thicknesses of SiO_2 films grown on silicon

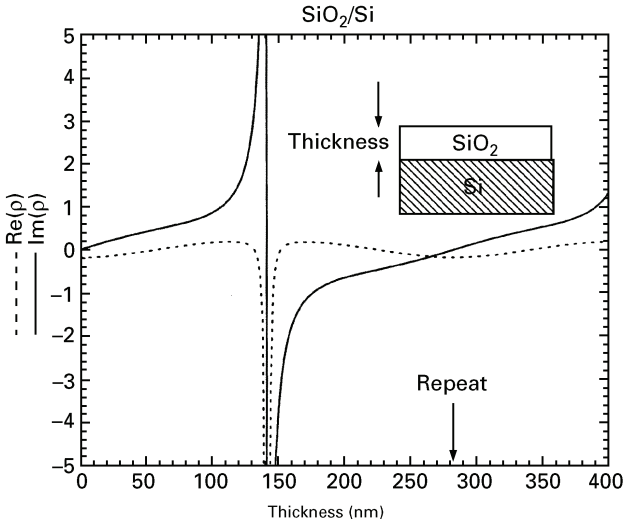

Figure 6 The complex reflection ratio ρ for the system described in **Figure 5**.

(66 nm, 190 nm and 321 nm) at an angle of incidence of 65°. There are several points where $\mathrm{Im}(\rho) = 0$ and where $-\mathrm{Re}(\rho)$ is a maximum: ~335 nm for the 66 nm film; ~305 nm for the 190 nm film; and ~315 nm and ~505 nm for the 321 nm film. Using spectroscopic ellipsometry for this system is similar to sampling several points along the ψ–Δ trajectory shown in **Figure 5**, although the precise values of the null points of $\mathrm{Im}(\rho)$ will not scale, since N_f and N_s are both functions of wavelength.

Spectroscopic ellipsometry data analysis

It is easy to see that there are more than 100 data points in each of **Figures 7A–C**, but only a few parameters to be determined from the data; the problem is overdetermined. Therefore, fitting procedures must be used to determine film thicknesses and other properties of thin films from spectroscopic ellipsometry. This process has three steps: (1) model the near-surface region of the sample; (2) parametrize or determine the optical functions of each layer; (3) fit the data using a realistic figure of merit to measure the 'goodness of fit'. For the case of SiO_2 grown on silicon, a four-media model is used, consisting of air/SiO_2/interface/silicon. The optical functions of the SiO_2 layer are assumed to follow the Sellmeier approximation:

$$n^2 = 1 + \frac{A\lambda^2}{\lambda^2 - \lambda_0^2} \qquad [13]$$

Table 1 The results of the fitting procedure on the spectroscopic ellipsometry data taken on several thin-film SiO_2/Si samples, shown in **Figures 7A–C**. The refractive index is calculated from Equation [13] assuming λ_0 = 92.3 nm

Sample	*Film thickness (nm)*	*A*	*Refractive index (600 nm)*	*Interface thickness (nm)*	χ^2
a	66.4 ± 0.1	1.149 ± 0.002	1.475	0.0 ± 0.2	0.18
b	188.9 ± 0.3	1.115 ± 0.003	1.464	1.4 ± 0.2	1.21
c	321.5 ± 0.4	1.139 ± 0.003	1.472	1.0 ± 0.2	0.84
Fused silica	–	1.099	1.458	–	–

where the two possible fitting parameters are the amplitude A and the resonance wavelength λ_0. The interface is assumed to be a thin layer whose optical functions are those of a Bruggeman effective medium, consisting of 50% SiO_2 and 50% Si, and the optical functions of silicon are taken from the literature. Using this model, three parameters are determined in the fitting procedure (listed in **Table 1**): the film thickness d_f, A from Equation [12] and the thickness of the interface $d_{interface}$; the resonant wavelength λ_0 = 92.3 nm. The third step of the analysis involves the actual fitting of the calculated values of ρ with the measured values of ρ. This can be done using a Levenberg–Marquardt algorithm to solve for the fitted parameters $d_{interface}$, d_f and A using the reduced χ^2 as the figure of merit:

$$\chi^2 = \frac{1}{N - m - 1} \sum_{i=1}^{N} \frac{(\rho_{exp}(\lambda_i) - \rho_{calc}(\lambda_i, \boldsymbol{z}))^2}{\delta\rho_{exp}^2(\lambda_i)} \qquad [14]$$

The sum in Equation [13] is taken over N wavelength points (λ_i), $\boldsymbol{z}$ is a vector of the fitted parameters (in this case, $d_{interface}$, d_f and A), and m is the dimensionality of $\boldsymbol{z}$ (i.e. 3). The quantities in the denominator ($\delta\rho_{exp}^2(\lambda_i)$) are the errors in the experimental data. The χ^2 is a good metric for the 'goodness of fit' to ellipsometry data. If χ^2 is near 1 the fit is a good fit, but if it is much greater than 1 the model does not fit the data. After the parameters are determined, it is also necessary to calculate the error limits as well as the correlation coefficients of all the fitted parameters.

The results of the fits to the data presented in **Figures 7A–C** are shown in **Table 1**, as well as the errors of each of the fitted parameters and the final χ^2 of the fit. All χ^2 values are near 1, indicating that the model fits the data. The errors listed for the thickness are all small, showing that the film thickness is a very well determined parameter for these data sets. The parameter A is a measure of the SiO_2 refractive index,

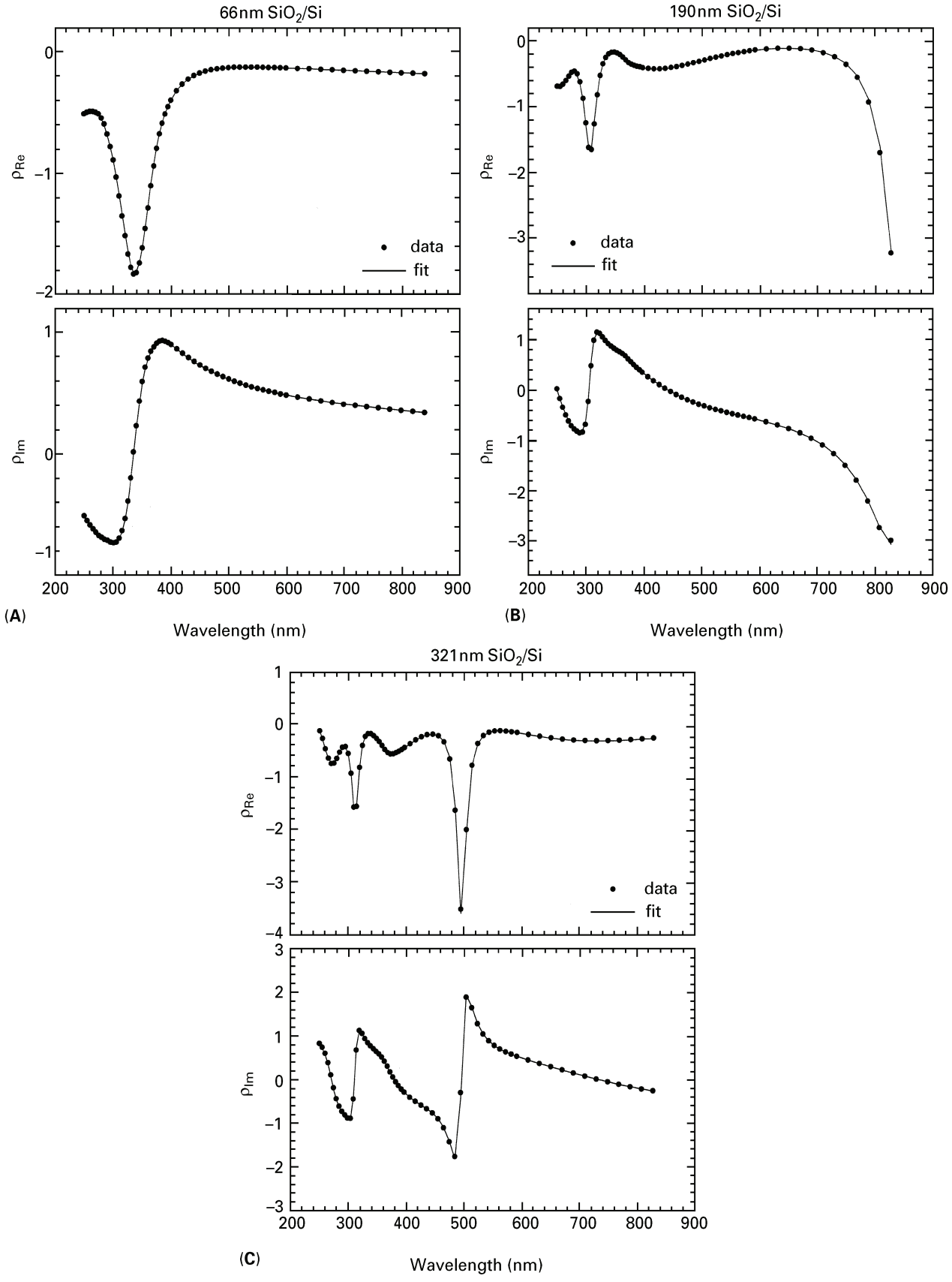

Figure 7 The spectroscopic values of the complex reflection ratio ρ for three samples of SiO_2 films grown on silicon as measured by spectroscopic ellipsometry. The three different thicknesses are (A) 66 nm, (B) 190 nm, and (C) 321 nm.

showing that thin-film SiO_2 can have a slightly larger refractive index than bulk fused silica.

List of symbols

A = Bessel angle of PEM modulation, amplitude; $C = \sin(2\psi)\cos(\Delta)$; d = film thickness; I_0 = total intensity element of Stokes vector; I_n = element of Stokes vector, intensity of light linearly polarized at n degrees; J_n = Bessel functions; $\mathbf{J}$ = Jones matrix; k = extinction coefficient; m = dimensionality of z; $\mathbf{M}$ = Mueller matrix, normalized Mueller–Jones matrix; $\mathbf{M}_{MJ}$ = Mueller–Jones matrix; n = refractive index; N_0, N_f, N_s = complex refractive indices; r_p, r_s, etc. = complex reflection coefficients; $S = \sin(2\psi)\sin(\Delta)$; $\boldsymbol{S}$ = Stokes vector; V = voltage, I_{rc}–I_{lc} element of Stokes vector; z = vector of fitted parameters (Eqn [14]); α = absorption coefficient; δ_c = constant phase shift; Δ = ellipsometry angle; θ = azimuthal angle; λ = wavelength; ρ = complex reflection ratio; ϕ = angle of incidence; ϕ_f, ϕ_s = complex angles; χ^2 = figure of merit; ψ = ellipsometry angle; ω = angular frequency.

See also: **Chiroptical Spectroscopy, Oriented Molecules and Anisotropic Systems; Fibres and Films Studied Using X-Ray Diffraction; Fluorescence Polarization and Anisotropy; Light Sources and Optics; Linear Dichroism Theory.**

Further reading

Azzam RMA (1995) *Ellipsometry*, In: Bass M (ed) *Handbook of Optics II*, Chapter 27. New York: McGraw-Hill.

Azzam RMA and Bashara NM (1987) *Ellipsometry and Polarized Light*. Amsterdam: Elsevier Science.

Chipman RA (1995) Polarimetry. In: Bass M (ed) *Handbook of Optics II*, Chapter 22. New York: McGraw-Hill.

Collins RW (1990) Automatic rotating element ellipsometers: calibration, operation, and real-time applications. *Review of Scientific Instruments* **61**: 2029–2062.

Drévillon B (1993) Phase modulated ellipsometry from the ultraviolet to the infrared: *in-situ* application to the growth of semiconductors. *Progress in Crystal Growth and Characterization of Materials* **27**: 1–87.

Hauge PS (1980) Recent developments in instrumentation in ellipsometry. *Surface Science* **96**: 108–140.

Jellison GE Jr (1993) Characterization of the near-surface region using polarization-sensitive optical techniques. In: Exharos GJ (ed) *Characterization of Optical Materials*, pp 27–47. Stoneham, MA: Butterworth-Heinemann.

Jellison GE (1998) Spectroscopic ellipsometry data analysis: measured vs. calculated quantities. *Thin Solid Films* **313–314**: 33–39.

Kliger DS, Lewis JW and Randall CE (1990) *Polarized Light in Optics and Spectroscopy*. New York: Academic Press.

Tompkins HG (1993) *A User's Guide to Ellipsometry*. New York: Academic Press.

Enantiomeric Purity Studied Using NMR

Thomas J Wenzel, Bates College, Lewiston, ME, USA

MAGNETIC RESONANCE
Applications

Introduction

Living organisms have a remarkable ability to distinguish enantiomers. Enzymes and cell surface receptors are handed, such that enantiomers often exhibit different properties in living systems. In extreme cases one enantiomer might be beneficial to a living organism, whereas the other might be harmful. Therefore, it is critical that methods exist to determine the enantiomeric purity and assign absolute configurations of chemical compounds. Various types of chiroptical spectroscopy are used for this. NMR spectroscopy is one of the most common and powerful methods for the determination of enantiomeric excess (typically to 1% of the minor enantiomer) and absolute configurations. There are generally considered to be three broad categories of reagents suitable for chiral resolution in NMR spectroscopy: chiral derivatizing agents, chiral solvating agents, and lanthanide shift reagents.

Chiral derivatizing agents are optically pure compounds that undergo reactions with the enantiomers being analysed. Most derivatization reactions involve the formation of covalent bonds; however, some examples, most notably with carboxylic acids and amines, rely on the formation of soluble salts.